# Detection and *In Situ* Switching of Unreversed Interfacial Antiferromagnetic Spins in a Perpendicular-Exchange-Biased System

Yu Shiratsuchi,[1,*] Hayato Noutomi,[1] Hiroto Oikawa,[1] Tetsuya Nakamura,[2] Motohiro Suzuki,[2] Toshiaki Fujita,[1] Kazuto Arakawa,[3,†] Yuichiro Takechi,[1] Hirotaro Mori,[3] Toyohiko Kinoshita,[2] Masahiko Yamamoto,[1] and Ryoichi Nakatani[1]

[1]*Department of Materials Science and Engineering, Graduate School of Engineering, Osaka University, 2-1 Yamada-oka, Suita, Osaka 565-0871, Japan*

[2]*Japan Synchrotron Radiation Research Institute (JASRI/SPring-8), 1-1-1 Kouto, Sayo, Hyogo 679-5198, Japan*

[3]*Research Center for Ultra-High Voltage Electron Microscopy, 7-1 Mihoga-oka, Ibaraki, Osaka 567-0047, Japan*

(Received 3 February 2012; published 16 August 2012)

By using the perpendicular-exchange-biased Pt/Co/$\alpha$-$Cr_2O_3$ system, we provide experimental evidence that the unreversed uncompensated Cr spins exist at the Co/$\alpha$-$Cr_2O_3$ interface. The unreversed uncompensated Cr spin manifests itself in both the vertical shift of an element-specific magnetization curve and the relative peak intensity of soft-x-ray magnetic circular dichroism spectrum. We also demonstrate an *in situ* switching of the interfacial Cr spins and correspondingly a reversal of the exchange bias without interfacial atomic diffusion. Such switching shows the direct relationship between the interfacial antiferromagnetic spins and origin of the exchange bias. The demonstrated switching of exchange bias would likely offer a new design of advanced spintronics devices, using the perpendicular-exchange-biased system, with low power consumption and ultrafast operation.

DOI: 10.1103/PhysRevLett.109.077202 PACS numbers: 75.70.Cn

Exchange bias is an effect that occurs at the interface of ferromagnetic (FM) and antiferromagnetic (AFM) layers. It is a long-standing issue in fundamental physics and also a crucial phenomenon that controls the magnetization direction in modern spintronics devices such as giant magnetoresistive heads [1]. The magnetization of an exchange-biased system is forced in a particular direction against a magnetic-field reversal [2–4]. This unidirectional nature of the system requires some symmetry-breaking of the interfacial spin structure. Although the theory predicts that this symmetry-breaking is caused by the interfacial uncompensated AFM spin which does not reverse with the magnetization reversal of the FM layer, its existence is still controversial in the intensively investigated Co(-Fe)/Mn-Ir(111) in-plane exchange-biased system [5–9]. In this system, the interfacial AFM spin possesses six-fold symmetry of in-plane orientations owing to 3Q spin density wave (T1-type) spin alignment for disordered $\gamma$-Mn-Ir ($L1_2$-$Mn_3Ir$) and the number of equivalent spin orientation increases statistically when the Mn-Ir(111) film is not a single crystal. In this rather typical case, the differently oriented unreversed interfacial AFM spins would be smeared out macroscopically. In this study, we address unreversed interfacial AFM spins by suppressing the orientation variation of the interfacial AFM spin. Perpendicular magnetization and perpendicular exchange bias (PEB) offer a good opportunity to achieve this aim because the spins are restricted to either up or down orientations relative to the surface normal. This bistability of spin orientation is not broken by magnetic domains and/or in-plane crystal orientations. In this paper, we provide evidence that the unreversed interfacial AFM spins indeed exist by using a Pt/Co/$\alpha$-$Cr_2O_3$/Pt perpendicular-exchange-biased system [10]. We further demonstrate *in situ* switching of both the interfacial AFM spins and the PEB. The *in situ* switching demonstrated is achieved using the $\alpha$-$Cr_2O_3$ thin film in contrast to the previous reports [11] using the bulk, which is essential for the device with high integration and low power consumption.

The sample was fabricated by using a DC magnetron sputtering method. The base pressure of the adopted system was below $7 \times 10^{-7}$ Pa. The fabricated sample consisted of Pt(1.0 nm)/Co(0.5 nm)/$\alpha$-$Cr_2O_3$(120 nm)/Pt(20 nm) grown on an $\alpha$-$Al_2O_3$(0001) substrate. Details of the preparation method are in our previous paper [10]. Structural characterizations were performed by *in situ* reflection high-energy electron diffraction (RHEED), x-ray diffraction, transmission electron microscopy (TEM), atomic force microscopy, x-ray photoelectron spectroscopy (XPS), and electron energy loss spectroscopy (EELS). Soft-x-ray absorption spectroscopy (XAS) and magnetic circular dichroism (XMCD) spectroscopy, which are element-specific techniques, were adopted to detect uncompensated Cr spins and separate tiny magnetic signals of the Cr spins from large signals of the Co layer [12]. The XAS and XMCD measurements were carried out at beam line BL25SU of the SPring-8 synchrotron radiation facility [13]. XMCD was obtained by the difference between the XAS for left and right circularly polarized x rays with a degree of circular polarization of $\pm 0.96$. Absorption signals were recorded by the total electron yield (TEY) method applying a bias voltage of $-18$ V. The helicity

 

of the circularly polarized x rays was switched at a rate of 1 Hz. The incident angle of the x rays was 10° from the surface normal. For all XMCD measurements, the magnetic field was applied to the out-of-plane direction. XAS and XMCD measurements were carried out at 180 and 235 K after cooling the sample in a perpendicular magnetic field of ±0.4 T from 315 K, which is above the Néel temperature of $\alpha$-$Cr_2O_3$ (307 K) [14].

Figure 1(a) shows a RHEED pattern of the $\alpha$-$Cr_2O_3$ layer. The pattern reflects the streaks with unequally spaced spots indexed by the $\alpha$-$Cr_2O_3(0001)$ layer. Observation of the lattice parameters and the valence state (not shown) supported the formation of the $\alpha$-$Cr_2O_3(0001)$ layer. Any other peaks except for $Cr^{3+}$ are not observed in the XPS profiles, suggesting that metal Cr, which would form the interfacial Co-Cr alloy, is not segregated in the film. From the RHEED patterns of the other layers—the Pt buffer, Co, and Pt capping layers—we confirmed that these are fcc(111) films. The sharp interfaces between the layers were and the well-ordered lattice periods are confirmed from cross-sectional TEM images shown in Fig. 1(b). The fast Fourier transform (FFT) image obtained from the $\alpha$-$Cr_2O_3(0001)$ layer shown in Fig. 1(c) indicates that the crystalline orientation is ⟨0001⟩ normal to the film. The different lattice period was observed at the different position of the $\alpha$-$Cr_2O_3$ layer (not shown), the crystal orientation in the growth direction is maintained to be ⟨0001⟩. According to the Cr spin alignment of a bulk $\alpha$-$Cr_2O_3$ [15], the Cr spins in the $\alpha$-$Cr_2O_3(0001)$ film align up or down relative to the surface normal. In principle, the Cr spins at the topmost surface of the $\alpha$-$Cr_2O_3(0001)$ layer can be fully uncompensated, but the surface roughness can compensate some interfacial Cr spins. In our case, a roughness of the $\alpha$-$Cr_2O_3(0001)$ surface without any overlayer was estimated to be ≈ 0.38 nm in root-mean-square value for a $1 \times 1$ $\mu m^2$ region by an atomic force microscopy. For the $\alpha$-$Cr_2O_3(0001)$ surface with a Co/Pt overlayer, an x-ray reflectivity analysis gave the Co/$\alpha$-$Cr_2O_3$ interfacial roughness value of ≈ 0.37 nm.

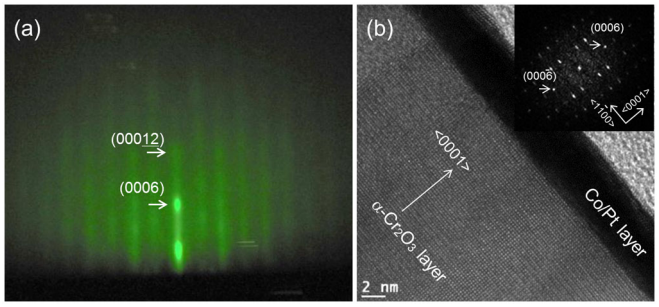


FIG. 1 (color online). (a) RHEED pattern of the $\alpha$-$Cr_2O_3(0001)$ layer. The azimuth direction of the electron incidence was [11$\bar{2}$0] of the $\alpha$-$Al_2O_3(0001)$ substrate. (b) Cross-sectional high-resolution TEM images. The direction of the electron incidence was [11$\bar{2}$0] of the $\alpha$-$Al_2O_3(0001)$ substrate. The inset shows the FFT image of the $\alpha$-$Cr_2O_3(0001)$ lattice.

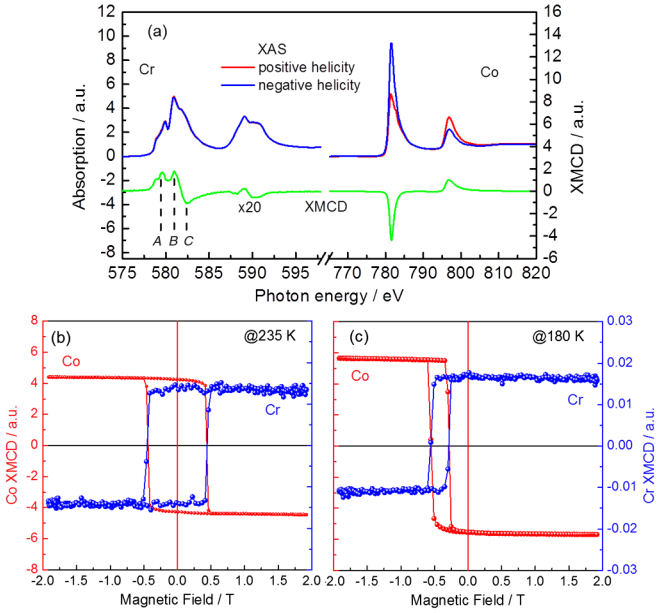


FIG. 2 (color online). (a) XAS, XMCD spectra measured at 180 K after cooling the sample in the +0.4 T magnetic field at Co $L_{2,3}$ and Cr $L_{2,3}$ edges. Red (black) and blue (dark gray) lines represent the absorption spectra for the positive and negative helicities, respectively, of the incident photons. Green (light gray) curves represent the XMCD spectrum. (b),(c) ESMCs for Co and Cr measured at (b) 235 K and (c) 180 K. Red small (blue large) lines represent the curves for Co (Cr), respectively. The ESMC for Co shown here is the difference curve at energy positions $L_3$ and $L_2$, and the ESMC for Cr is the difference curve at energy positions $B$ and $C$ labeled in the XMCD spectrum.

Figure 2(a) shows the XAS and XMCD spectra for the Co $L_{2,3}$ and Cr $L_{2,3}$ edges at 180 K. Measurements were performed after cooling the sample in the perpendicular magnetic field of +0.4 T. The XAS of Co shows a metallic feature and a minute amount of Co oxidation. For comparison, oxygen was not detected by EELS at the Co/$\alpha$-$Cr_2O_3$ interface of a similar sample using a 5.0-nm-thick Pt capping layer [16]. Thus, we believe that the topmost Co layer could be oxidized due to the very thin Pt capping layer, but a possibility of an intrinsic interfacial oxidation/reduction cannot be ruled out [17]. The XAS of Cr is similar to the reported spectrum for $\alpha$-$Cr_2O_3$ [18,19] with multiplet structures. XMCD signals were clearly observed at both the Co $L_{2,3}$ and the Cr $L_{2,3}$ edges. We assert that the Cr XMCD signal supports the presence of uncompensated Cr spins at the interface with Co. No XMCD signal at the Cr $L_{2,3}$ edges was detected in a film without a Co layer (not shown). Additionally, the magnetic-field dependence of the XMCD intensity of Cr followed that of Co, as shown later. These results indicate that the uncompensated Cr spins are induced by the interfacial exchange coupling with Co. The reported XMCD spectrum from a surface magnetization domain of bulk $Cr_2O_3$ does not show the multiplet structure and its shape resembles the XMCD spectrum of a metal ferromagnet [20]. In contrast,

the shape of our XMCD spectrum of Cr is similar to that of $Cr^{3+}$ in Cr charcogenides [21] and does not resemble to those of $Cr^{4+}$ in FM Cr oxides [22] or Cr clusters [23]. Considering the influence of a crystal field on XAS and XMCD spectrum [18,21], the prominent peak labeled $A$ in Fig. 2(a) suggests a strong crystal field at the $Cr^{3+}$ site from the $O^{2-}$ lattice.

We estimated the effective spin magnetic moment, $m_s^{\text{eff}} = m_s + 7\langle T_z \rangle$, and the orbital magnetic moment $m_l$ using the XAS and XMCD spectra by sum-rule analyses [24,25], where $m_s$ is the pure spin magnetic moment and $\langle T_z \rangle$ is the expectation value of the magnetic dipole operator. The resulting values are $m_s^{\text{eff}} = 1.79 \pm 0.13\mu_B$ and $m_l = 0.16 \pm 0.04\mu_B$ for Co, and $m_s^{\text{eff}} = -0.16 \pm 0.04\mu_B$ and $m_l < \pm 0.002\mu_B$ for Cr. In the analysis, we assumed the number of 3d holes $n_h = 2.45$ for Co [26] and $n_h = 7.0$ for Cr [27], and the spin correction factor SC = 1.68 for Cr, a light 3d element [28]. The obtained $m_s^{\text{eff}}$ values have opposite signs for Co and Cr, indicating the AFM exchange coupling between Co and Cr spins [12]. Note that the $m_s^{\text{eff}}$ values may include a considerable contribution of the $7\langle T_z \rangle$ term as large as a few tens percent owing to anisotropic local environments of the ultrathin Co layer ($\sim 2$ ML) and the uniaxial crystal structure of $\alpha$-$Cr_2O_3$. From the measured magnetic moment values of Cr, the proportion of the uncompensated interfacial Cr spins can be estimated to be $0.57 \pm 0.13$ per monolayer. A significant spin imbalance should be present at the Co/$\alpha$-$Cr_2O_3$ interface and, namely, half of the interfacial Cr atoms should possess a net magnetic moment. In the estimation, we used the typical electron escape length of 2.0 nm for TEY detection [29] and the reported magnetic moment ($2.48\mu_B$) of $Cr^{3+}$ in $\alpha$-$Cr_2O_3$ [30] and assumed that all uncompensated Cr moments were localized at one monolayer of the interface. In the FM/Mn-Ir in-plane exchange-biased system, it was reported that the uncompensated AFM spins were caused by the rotation of interfacial AFM spins from the original spin orientation in bulk Mn-Ir [9]. In the FM/$\alpha$-$Cr_2O_3$(0001) perpendicular-exchange-biased system, the broken equivalence of the oppositely directed magnetic domains also causes the uncompensated fraction of the interfacial AFM spins. This mechanism is consistent with the previously proposed surface magnetization or the boundary magnetization [31].

We determined magnetic hysteresis loops separately for the Co spins and for the uncompensated Cr spins by element-specific magnetization curve (ESMC) measurements. As-measured ESMC using the TEY detection exhibited artificial dips around zero fields: approximately 7% for Co with respect to the XMCD signal at saturated magnetization but negligibly small for Cr. In the following, we show a ratio of the XMCD intensity to the spin-averaged XAS intensity, $2(I^+ - I^-)/(I^+ + I^-)$ to eliminate the artificial dip, where $I^+(I^-)$ denotes a TEY signal for x-ray helicitiy parallel (antiparallel) to the x-ray wave vector [13]. Figure 2(b) compares ESMCs of Co and Cr at 235 K. The ESMC of Cr plots a difference of the XMCD values measured at the energy positions $B$ and $C$ in Fig. 2(a). At 235 K, the ESMCs of both Co and Cr are symmetric and not shifted along either the vertical (magnetization) or the horizontal (external field) axis. An abrupt onset of the PEB was observed just below 235 K, accompanied with the decrease of the coercivity, which can be explained by the Meilkejohn and Bean's exchange anisotropy model [2,10,32]. At 180 K, the center of the hysteresis loops was shifted by $-0.4$ T toward negative fields due to the PEB [Fig. 2(c)]. The observed PEB field gives a unidirectional magnetic anisotropy energy of $0.42\ \text{mJ/m}^2$. Despite the AFM interfacial coupling, a negative exchange bias was observed owing to the low cooling field adopted [33]. In addition to the horizontal shift of the loops due to the exchange bias, we observed a characteristic shift of the ESMC along the vertical axis only in Cr at 180 K. Figure 2(c) demonstrates a clear shift of the ESMC of Cr along the vertical axis, whereas the ESMC of Co does not. The vertical shift is about 25% of the total XMCD signal that corresponds to the net magnetization of the uncompensated Cr spins.

We show that the sign of the vertical shift of the ESMC of Cr can be reversed by changing the cooling-field direction. The results in Figs. 2(a)–2(c) were obtained for the sample that had been cooled in a positive magnetic field of $+0.4$ T. After these measurements, the sample was once heated up to 315 K (i.e. above the Néel temperature) and subsequently recooled down to 235 K and 180 K in a negative magnetic field of $-0.4$ T. Figures 3(a) and 3(b) show the ESMCs of Cr measured at the aforementioned energy position $B$. At 235 K, the ESMCs for the positive- and negative-cooling-fields are identical and show no shifts [Fig. 3(a)]. Upon switching on of the exchange bias, reversed shifts were observed in both the horizontal and the vertical axes [Fig. 3(b)]. The amount of the vertical shift is the same for both cooling-field directions.

The vertical shift of the ESMCs is direct evidence of the presence of unreversed uncompensated Cr spins and asymmetry of the XMCD spectra has also evidenced their presence. Figures 3(c) and 3(d) show XMCD spectra of Cr for the cooling-field of $\pm 0.4$ T. The unreversed uncompensated Cr spin manifests itself in the relative intensity of the peaks labeled $A$ and B. For positive-field-cooling, peak $B$ is higher (lower) than peak $A$ at $+1.0$ ($-1.0$) T and vice versa for negative-field-cooling. Note that $\pm 1.0$ T is sufficiently high for the magnetization reversal of the FM layer. Since the XMCD signal is proportional to the spin projection to the magnetic-field axis, the vertical shift and the change in the XMCD intensity indicate the presence of uncompensated Cr spins whose direction does not follow a reversal of Co magnetization.

A vertical shift was often interpreted as a pinned faction of the uncompensated AFM spins [5]. In this "pinned spin model," since the pinned spin is strictly fixed to the original orientation, the XMCD spectrum from the pinned spins should be identical for the magnetic-field reversal, which disagrees with our experimental results. Besides, the

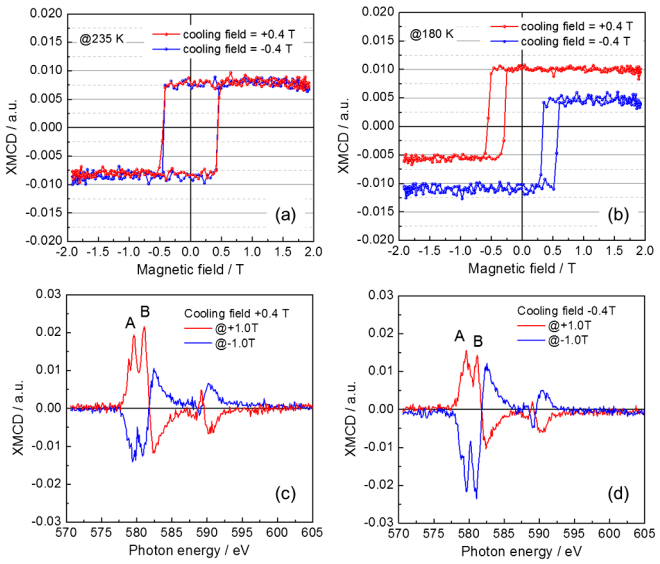


FIG. 3 (color online). ESMCs for Cr $L_3$ edge measured at (a) 230 K and (b) 180 K. Red (black) and blue (dark gray) curves correspond to the curves acquired after cooling the sample in the positive and negative fields, respectively. XMCD spectrum for Cr $L_{2,3}$ edges measured at 180 K after cooling the sample in the (c) positive and (d) negative magnetic fields. Red (black) and blue (dark gray) curves correspond to the spectra measured at $+1.0$ T and $-1.0$ T, respectively.

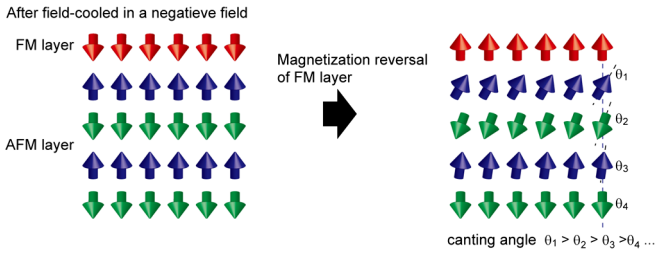


FIG. 4 (color online). Left figure represents the spin configuration after the field-cooling in the negative magnetic field. Right figure represents the spin configuration after the FM magnetization reversal. Red or dark gray arrows represent the FM spins. Blue or black (green or light gray) arrows represent the up (down) AFM spins. The dotted lines in the right figure represent the original orientation of the AFM spins. $\theta_i$ $(i = 1, 2, 3 \ldots)$ represents the canting angle of the AFM spin.

pinned spin model assumes that all uncompensated AFM spins are unpinned above the blocking temperature and a fraction of the uncompensated AFM spins is pinned below the blocking temperature and that these two types of AFM spins assume the coercivity enhancement and the exchange bias, respectively. In our system, as shown in Figs. 2(b) and 2(c), the coercivity decreases steeply by one-fourth accompanied by the onset of the exchange bias. Although this steep decrease of the coercivity implies that the 75% of the uncompensated Cr spins are pinned, this value is very large compared to the reported value (3–4%) [5,34] and such a large amount of the pinned spins would generate a more significant vertical shift than the observed value.

Here, we discuss the spin structure at the Co/$\alpha$-$Cr_2O_3$ interface, introducing a model in which the Cr spins are supposed to cant. Figure 4 shows a spin configuration considered in our model. Perfect interface without the interface roughness has been assumed. After the field-cooling in the negative field, all Co spins align down and the interfacial Cr spins align up owing to the AFM interfacial exchange coupling between Co and Cr. When the FM magnetization reverses by the external magnetic field, the interfacial Cr spins cant from the original direction to keep the AFM configuration with the Co spins. The interfacial Cr spin need not reverse or flip because the magnetic anisotropy of $\alpha$-$Cr_2O_3$ restricts the Cr spin in either up or down below the onset temperature of PEB [10]. The interfacial AFM spin canting can be promoted by the interfacial roughness [35]. Since the exchange coupling energy is proportional to the scalar product of FM and AFM spin vectors, this spin canting can cause the symmetry-breaking of the interfacial spin structure which generates the exchange bias [36]. In this model, the hysteresis and the vertical shift of the ESMC are caused by the spin canting and the unflipped nature of the uncompensated AFM spin, respectively. When the interface becomes flat, the vertical shift increases owing to increasing interfacial Cr spin imbalance. When the proportion of up and down spins is equivalent, for example when the interface is rough, the interfacial AFM spins are compensated; hence, the oppositely directed vertical shifts are canceled out. The exchange bias in the rough interface should be treated by the model proposed by Malozemoff [37]. The FM alignment of Cr spins in the $c$ plane promotes the appearance of the vertical shift. If the AFM spins had an alternating spin arrangement in the in-plane unit cell, the vertical shift would be weakened because the proportion of interfacial up and down spins is almost the same. In the case that the AFM spin possesses more than three orientations owing to a noncollinear spin alignment such as that in Mn-Ir(111) [8,9], the vertical shift would be smeared out at the macroscopic scale.

The neutron and x-ray reflectivity study revealed that the pinned uncompensated AFM spins extend in the bulk site of the AFM layer [34,38,39]. In our model, this effect corresponds to the spin canting extended into the bulk site of the AFM layer. As the canting angle deceases with increasing distance from the interface, the frustrated spin structure such as the magnetic domain [38] is generated in the AFM layer. The finite width of this frustrated spin structure would be related to the critical thickness of the AFM layer [40].

In summary, we have observed the vertical shift of ESMC of Cr and the change in the peak intensity of the XMCD spectrum with the magnetic-field direction in the perpendicular-exchange-biased Pt/Co/$\alpha$-$Cr_2O_3$ system. The possible interfacial spin configuration to explain the results are discussed, in which the interfacial AFM spins need not flip with the FM magnetization reversal. We also demonstrated the *in situ* switching of the uncompensated Cr

spins, which may offer the new design of spintronics devices with low power consumption and ultrafast operation.

Y. S. would like to thank Dr. A. Sugihara from Osaka University for the help of XAS and XMCD measurements, Professor S. Fujimoto from Osaka University for XPS measurements, Dr. C. Mitsumata and Dr. M. Tsunoda from Tohoku University for the useful discussion. The XAS and XMCD experiments were performed at SPring-8 with the approval of Japan Synchrotron Radiation Research Institute (JASRI) (Proposal Nos. 2011A1172 and 2011B1707). This study was partly supported by the Priority Assistance for the Formation of Worldwide Renowned Centers of Research—The Global COE Program (Project: Center of Excellence for Advanced Structural and Functional Materials Design) from the Ministry of Education, Culture, Sports, Science and Technology (MEXT), Japan, and by the Murata Science Foundation.

*Corresponding author.
shiratsuchi@mat.eng.osaka-u.ac.jp
†Present address: Department of Material Science, Interdisciplinary Faculty of Science and Engineering, Shimane University, 1060 Nishikawazu-cho, Matsue, Shimane 690-8504, Japan.

[1] C. Chappert, A. Fert, and F. Nguyen Van Dau, Nature Mater. **6**, 813 (2007).
[2] W. H. Meiklejohn and C. P. Bean, Phys. Rev. **102**, 1413 (1956); **105**, 904 (1957).
[3] J. Nogués and I. K. Shuller, J. Magn. Magn. Mater. **192**, 203 (1999).
[4] A. E. Berkowitz and K. Takano, J. Magn. Magn. Mater. **200**, 552 (1999).
[5] H. Ohldag, A. Scholl, F. Nolting, E. Arenoholtz, S. Maat, A. T. Young, M. Carey, and J. Stöhr, Phys. Rev. Lett. **91**, 017203 (2003).
[6] M. Tsunoda, T. Nakamura, M. Naka, S. Yoshitaki, C. Mitsumata, and M. Takahashi, Appl. Phys. Lett. **89**, 172501 (2006).
[7] S. Doi, N. Awaji, K. Nomura, T. Hirono, T. Nakamura, and H. Kimura, Appl. Phys. Lett. **94**, 232504 (2009).
[8] M. Tsunoda, H. Takahashi, T. Nakamura, C. Mitsumata, S. Isogami, and M. Takahashi, Appl. Phys. Lett. **97**, 072501 (2010).
[9] H. Takahashi, Y. Kota, M. Tsunoda, T. Nakamura, K. Kodama, A. Sakuma, and M. Takahashi, J. Appl. Phys. **110**, 123920 (2011).
[10] Y. Shiratsuchi, T. Fujita, H. Oikawa, H. Noutomi, and R. Nakatani, Appl. Phys. Express **3**, 113001 (2010).
[11] X. He, Y. Wang, N. Wu, A. N. Caruso, E. Vescovo, K. D. Belashchenko, P. A. Dowben, and Ch. Binek, Nature Mater. **9**, 579 (2010) and supplemental information.
[12] P. Borisov, T. Eimüller, A. Fraile-Rodríguez, A. Hochstrat, X. Chen, and W. Kleemann, J. Magn. Magn. Mater. **310**, 2313 (2007).
[13] T. Nakamura, T. Muro, F. Z. Guo, T. Matsushita, T. Wakita, T. Hirono, Y. Takeuchi, and K. Kobayashi, J. Electron Spectrosc. Relat. Phenom. **144-147**, 1035 (2005).
[14] D. N. Astrov, Zh. Eksp. Teor. Fiz. **40**, 1035 (1961) [Sov. Phys. JETP **13**, 729 (1961)].
[15] L. M. Corliss, J. M. Hastings, R. Nathans, and G. Shirane, J. Appl. Phys. **36**, 1099 (1965).
[16] Y. Shiratsuchi *et al.* (unpublished).
[17] H. Ohldag, T. J. Regan, J. Stöhr, F. Nolting, J. Lüning, C. Stamm, S. Anders, and R. L. White, Phys. Rev. Lett. **87**, 247201 (2001).
[18] G. van der Laan, and B. T. Thole, Phys. Rev. B **43**, 13401 (1991).
[19] Y. Yamazaki, T. Kataoka, V. R. Singh, A. Fujimori, F.-H. Chang, D.-J. Huang, H.-J Lin, K. Ishikawa, K. Zhang, and S. Kuroda, J. Phys. Condens. Matter **23**, 176002 (2011).
[20] N. Wu, X. He, A. L. Aleksander, L. Wysocki, U. Lanke, T. Kemesu, K. D. Belashchenko, Ch. Binek, and P. A. Dowben, Phys. Rev. Lett. **106**, 087202 (2011).
[21] A. Kimura, J. Matsuno, J. Okabayashi, A. Fujimori, T. Shishidou, E. Kulatov, and T. Kanomata, Phys. Rev. B **63**, 224420 (2001).
[22] E. Goering, A. Bayer, S. Gold, G. Schütz, M. Rabe, U. Rüdiger, and G. Günterrodt, Phys. Rev. Lett. **88**, 207203 (2002).
[23] C. Boeglin, P. Ohresser, R. Decker, H. Bulou, F. Scheurer, I. Chado, S. S. Dhesi, E. Gaudry, and B. Lazarovitz, Phys. Status Solidi B **242**, 1775 (2005).
[24] B. T. Thole, P. Carra, F. Sette, and G. van der Laan, Phys. Rev. Lett. **68**, 1943 (1992).
[25] P. Carra, B. T. Thole, M. Altarelli, and X. Wang, Phys. Rev. Lett. **70**, 694 (1993).
[26] N. Nakajima, T. Koike, T. Shidara, H. Miyauchi, H. Fukutani, A. Fujimori, K. Iio, T. Katayama, M. Nývlt, and Y. Suzuki, Phys. Rev. Lett. **81**, 5229 (1998).
[27] S. Watanabe, T. Nagasaki, and K. Ogasawara, J. Appl. Phys. **110**, 123524 (2011).
[28] E. Goering Philos. Mag. **85**, 2895 (2005).
[29] R. Nakajima, J. Stöhr, and Y. U. Idzerda, Phys. Rev. B **59**, 6421 (1999).
[30] P. J. Brown, J. B. Forsyth, E. Leliévre-Berna, and F. Tasset, J. Phys. Condens. Matter **14**, 1957 (2002).
[31] K. D. Blashchenko, Phys. Rev. Lett. **105**, 147204 (2010).
[32] M. Tsunoda, Y. Tsuchiya, T. Hashimoto, and M. Takahashi, J. Appl. Phys. **87**, 4375 (2000).
[33] J. Nogués, D. Lederman, T. J. Moran, and I. K. Schuller, Phys. Rev. Lett. **76**, 4624 (1996).
[34] M. R. Fitzsimmons, B. J. Kirby, S. Roy, Zhi-Pan Li, I. V. Roshchin, S. K. Sinha, and I. K. Schuller, Phys. Rev. B **75**, 214412 (2007).
[35] E. Jiménez, J. Camarero, J. Sort, J. Nogués, N. Mikuszeit, J. M. García-Martín, A. Hoffmann, B. Dieny, and R. Miranda, Phys. Rev. B **80**, 014415 (2009).
[36] C. Mitsumata, A. Sakuma, and K. Fukamichi, Phys. Rev. B **68**, 014437 (2003).
[37] A. P. Malozemoff, J. Appl. Phys. **63**, 3874 (1988).
[38] S. Roy, M. R. Fitzsimmons, S. Park, M. Dorn, O. Petracic, I. V. Roshchin, Zhi-Pan Li, X. Battle, R. Morales, A. Misra, X. Zhang, K. Chesnel, J. B. Kortright, S. K. Sinha, and I. V. Schuller, Phys. Rev. Lett. **95**, 047201 (2005).
[39] S. Brück, G. Schütz, E. Goering, X. Ji, and K. M. Krishnan, Phys. Rev. Lett. **101**, 126402 (2008).
[40] C. Mitsumata, A. Sakuma, K. Fukamichi, M. Tsunoda, and M. Takahashi, J. Phys. Soc. Jpn. **77**, 044602 (2008).